(*20*). By analogy with dopamine's effect on teleost horizontal cells (*21, 22*), dopamine release in the IPL may also alter the electrical coupling among AIIs and between AIIs and cone bipolar cells, thereby regulating the passage of rod signals to ganglion cells (*14*).

The present results suggest that the boutons along the axon-like component provide the synaptic connection between the DA amacrine and the AII amacrine cells (Fig. 3D). Moreover, the unique structure of the DA amacrine cell provides a clue to the function of this synapse; the morphology of the axon-like processes indicates a significant convergence of input from DA amacrines onto the AII amacrines. The magnitude of this convergence, given by dividing the estimated number of DA boutons per square millimeter (20,000 to 200,000) by the known density of AII amacrine cells (500 to 5,000) (*23*) could be as high as 40 boutons per AII amacrine. Their en passant location along the long axon-like processes indicates that each of these 40 boutons could originate from a different DA amacrine. Conversely, the boutons from a single DA amacrine must diverge to contact as many as 1800 AII amacrine cells.

Understanding the biological significance of such convergent-divergent neuronal geometry requires, in part, discovery of the function of the axon-like process. The striking transition from the thick, proximal dendrite to the thin, axon-like process may act as a high-resistance bottleneck, electrically isolating two parts of the dendritic tree. This would be analogous to those horizontal cells that have thin, axon-like processes that serve not to conduct action potentials but to prevent the passive spread of current between two independent dendritic systems (*24*). If this were the case, the DA boutons could operate independently, as local input-output units (*25, 26*). However, this hypothesis is not supported by electron microscopic studies that have found DA boutons in the IPL to be presynaptic only, resembling typical axonal synapses (*2–4*). Alternatively, the transition from dendritic to axon-like process may be equivalent to an axon hillock and may function as the site for initiation of an action potential that travels along the axon-like process. Dendritic action potentials occur in retinal amacrine cells (*27–29*), and in turtle retina the physiological effects of dopamine on horizontal cells can be mimicked by veratridine, a releaser of transmitter from the terminals of spike-generating neurons and prevented by tetrodotoxin, a blocker of voltage-gated Na^+ channels (*30*). The possibility that DA amacrine cells can transmit information laterally over long distances via an excitable axon suggests a synaptic mechanism by which global changes in illumination during light and dark adaptation could influence local changes in ganglion-cell receptive-field sensitivity.

REFERENCES AND NOTES

1. S. C. Mangel and J. E. Dowling, *Proc. R. Soc. London Ser. B* **231**, 91 (1987); T. Teranishi, K. Negishi, S. Kato, *J. Neurosci.* **4**, 1271 (1984).
2. J. E. Dowling and B. Ehinger, *J. Comp. Neurol.* **180**, 203 (1978).
3. I. Holmgren, *Invest. Ophthalmol. Vis. Sci.* **22**, 8 (1982).
4. R. G. Pourcho, *Brain Res.* **252**, 101 (1982).
5. A. Ames III and F. B. Nesbett, *J. Neurochem.* **37**, 867 (1981).
6. D. I. Vaney, *Science* **233**, 444 (1986).
7. A. Björklund, A. S. Horn, H. G. Baumgarten, A. Nobin, H. G. Schlossberger, *Acta Physiol. Scand. Suppl.* **429**, 29 (1975).
8. C. R. Creveling and A. Rotman, *Ann. N.Y. Acad. Sci.* **305**, 57 (1978).
9. B. Ehinger, *Z. Zellforsch. Mikrosk. Anat.* **71**, 146 (1966).
10. C. Versaux-Botteri *et al.*, *J. Comp. Neurol.* **243**, 422 (1986).
11. N. C. Brecha, C. W. Oyster, E. S. Takahashi, *Invest. Ophthalmol. Vis. Sci.* **25**, 66 (1984).
12. K. Negishi, T. Teranishi, S. Kato, *Neurosci. Lett.* **45**, 27 (1984).
13. J. Nyguyen-Legros, C. Botteri, P. Le Hoang, A. Vigny, M. Gay, *Brain Res.* **295**, 145 (1984).
14. A. P. Mariani, H. Kolb, R. Nelson, *ibid.* **322**, 1 (1984).
15. J. M. Frederick, M. E. Rayborn, A. M. Laties, D. M. K. Lam, J. G. Hollyfield, *J. Comp. Neurol.* **210**, 65 (1982).
16. I. Törk and J. Stone, *Brain Res.* **169**, 261 (1979).
17. C. W. Oyster, E. S. Takahashi, M. Cilluffo, N. C. Brecha, *Proc. Natl. Acad. Sci. U.S.A.* **82**, 6335 (1985).
18. Intracellular injections of LY under direct microscopic control have been used to determine the morphology of catecholaminergic amacrine cells that have been identified in fixed tissue after formaldehyde-induced histofluorescence in rabbit [M. Tauchi and R. H. Masland, *Soc. Neurosci. Abstr.* **12**, 57 (1986)] and cat retina (*19*). These studies demonstrated a similar pattern of proximal dendritic morphology but failed to detect the long axon-like processes described in this report. Voigt and Wässle acknowledged that the use of LY in fixed tissue does not clearly reveal the cell's finest processes and that the injected cells were understained.
19. T. Voigt and H. Wässle, *J. Neurosci.* **7**, 4115 (1987).
20. E. V. Famiglietti and H. Kolb, *Brain Res.* **84**, 293 (1975).
21. E. M. Lasater and J. E. Dowling, *Proc. Natl. Acad. Sci. U.S.A.* **82**, 3025 (1985).
22. T. Teranishi, K. Negishi, S. Kato, *Nature* **301**, 243 (1983).
23. D. I. Vaney, *Proc. R. Soc. London Ser. B* **224**, 475 (1985).
24. R. Nelson, A. V. Lützow, H. Kolb, P. Gouras, *ibid.* **189**, 137 (1975).
25. S. A. Elias and J. K. Stevens, *Brain Res.* **196**, 365 (1980).
26. R. F. Miller and S. A. Bloomfield, *Proc. Natl. Acad. Sci. U.S.A.* **80**, 3069 (1983).
27. F. S. Werblin and J. E. Dowling, *J. Neurophysiol.* **32**, 339 (1969).
28. R. F. Miller and R. F. Dacheux, *Brain Res.* **104**, 157 (1976).
29. S. Barnes and F. Werblin, *ibid.* **406**, 233 (1987).
30. M. Piccolino, P. Witkovsky, C. Trimarchi, *J. Neurosci.* **7**, 2273 (1987).

31. I thank T. Famiglietti, K. A. Mulligan, R. W. Rodieck, C. J. Shatz, and P. S. Ulinksi for helpful comments on the text and R. W. Rodieck for providing the space and guidance necessary to carry out this study. I thank M. Clarke, M. Watanabe, and T. Haun who provided assistance during the experiments. Supported by NIH grant EY 06678.

4 January 1988; accepted 31 March 1988

Calicheamicin γ_1^I: An Antitumor Antibiotic That Cleaves Double-Stranded DNA Site Specifically

NADA ZEIN, ACHYUT M. SINHA,* WILLIAM J. MCGAHREN, GEORGE A. ELLESTAD

Calicheamicin γ_1^I is a recently discovered diyne-ene–containing antitumor antibiotic with considerable potency against murine tumors. In vitro, this drug interacts with double-helical DNA in the minor groove and causes site-specific double-stranded cleavage. It is proposed that the observed cleavage specificity is a result of a unique fit of the drug and DNA followed by the generation of a nondiffusible 1,4-dehydrobenzene–diradical species that initiates oxidative strand scission by hydrogen abstraction on the deoxyribose ring. The ability of calicheamicin γ_1^I to cause double-strand cuts at very low concentrations may account for its potent antitumor activity.

CALICHEAMICIN γ_1^I (STRUCTURE 1) (*1, 2*) has been recently isolated from fermentations of *Micromonospora echinospora* ssp. calichensis and is a member of a newly discovered class of natural products (*3, 4*) found to be unusually potent antitumor agents. It is approximately 1000-fold more active than adriamycin against murine tumors and is optimal at 0.5 to 1.5 μg per kilogram of body weight (*5*). The high potency of calicheamicin γ_1^I in the biochemical assay of prophage induction (*6*) (active at picogram per milliliter concentrations) suggested that its activity was due to its ability to damage DNA. In addition, the drug can also cause chromosome aberrations

Infectious Disease Research Section, American Cyanamid Company—Medical Research Division, Lederle Laboratories, Pearl River, NY 10965.

*Present address: Genentech Inc., South San Francisco, CA 94080.

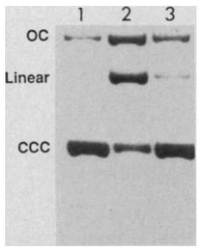

Fig. 1. Cleavage of ϕX174 replicative form I DNA with calicheamicin γ_1^I analyzed on a 1% agarose gel. The drug (1 μg of a solution of either 1 or 0.1 μg/ml) was incubated with the DNA (0.1 μg) and 10 m*M* β-mercaptoethanol in 10:90 dimethylsulfoxide:50 m*M* tris-HCl, *p*H 7.5 at 37°C for 15 min in a total reaction volume of 10 μl. The reaction mixture was loaded directly on a 1% agarose gel with subsequent ethidium bromide staining. Lane 1, DNA control; lane 2, calicheamicin γ_1^I at 0.1 μg/ml; lane 3, calicheamicin γ_1^I at 0.01 μg/ml. OC, open circle; CCC, covalently closed circle (supercoil).

in human diploid lung fibroblasts (*7*) and mutagenesis in *Escherichia coli* (*8*).

Calicheamicin γ_1^I contains several unusual structural features, including a glycosylated hydroxylamino sugar and a labile methyltrisulfide grouping that, upon reduction with thiols, initiates aromatization of the diyne-ene moiety via a 1,4-dehydrobenzene–diradical (*2*). It is believed that this diradical species (structure **2**) is responsible for the DNA damaging properties and cytotoxicity of calicheamicin. We report here that calicheamicin γ_1^I causes site-specific double-stranded (ds) DNA scission in vitro with different cleaving mechanisms for each strand.

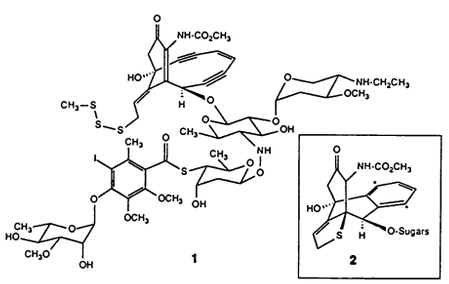

In the presence of thiol cofactors, calicheamicin γ_1^I at concentrations as low as 0.01 μg/ml (7 n*M*) causes ds and single-strand breaks in supercoiled ϕX174 DNA, as evidenced by the formation of linear and open-circular forms, respectively (Fig. 1). In the absence of thiol cofactors, only slight cutting was observed at 0.1 μg/ml. At 0.1 μg/ml, single-strand ϕX174 (+ strand) was unaffected by the drug, indicating the preference of calicheamicin γ_1^I for ds DNA.

To determine the specificity of the strand cleavage, we examined the reaction of calicheamicin γ_1^I with several 5′ end-labeled restriction fragments obtained from PUC 18 and from cloned *Streptomyces* promoter regions (*9*). Comparison of the electrophoretic mobility of the drug-induced cleavage products with the markers produced by the Maxam-Gilbert sequencing reactions (*10*) indicated that, in the presence of thiols, calicheamicin γ_1^I causes strand breaks 3 bp apart in the two DNA strands at specific sites. Without exception, the preferred site of attack was the 5′ C (3′ to the adjacent thymidine) of a TCCT sequence (Fig. 2A) and three nucleotides toward the 3′ side of the 3′ G in the complementary AGGA box (Fig. 2B). Other sites such as GCCT, TCCG, TCCC, CTCT (Fig. 2B), TCTC, ACCT, TCCA, and their complementary

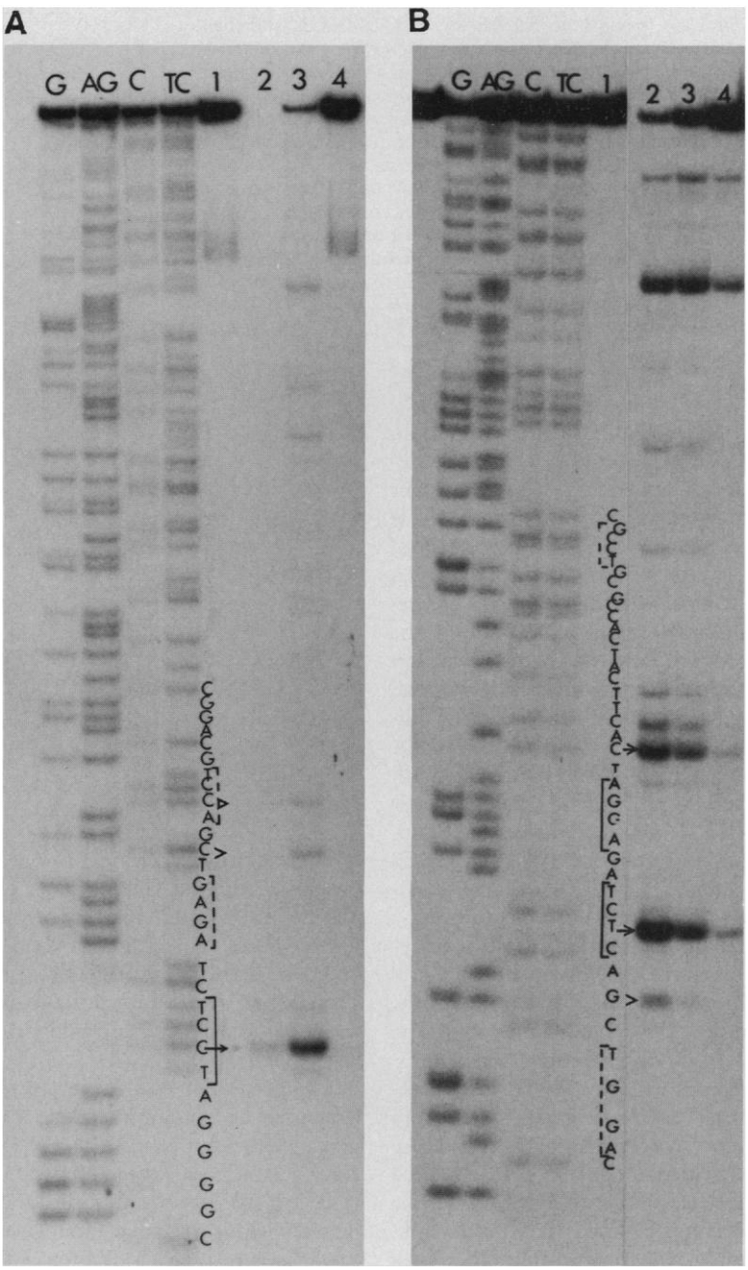

Fig. 2. Autoradiograms of high-resolution denaturing gel of calicheamicin γ_1^I cleavage of restriction fragments labeled at the 5′ end with ^{32}P. Reaction conditions were 10:90 dimethylsulfoxide:50 m*M* tris-HCl, *p*H 7.5, carrier calf thymus DNA at 5 μg/ml [20*M* excess (in base pairs) to the drug], 10 m*M* β-mercaptoethanol, and end-labeled DNA (≈6000 cpm) in a total volume of 50 μl. Reactions were run for 15 min at 37°C, then the DNA was ethanol-precipitated and washed. Cleavage products were analyzed on a 12% polyacrylamide sequencing gel at 1200 V for 3 hours. G, AG, C, and TC are Maxam-Gilbert chemical sequencing lanes. (**A**) Cleavage of 144-bp fragment Eco RI–Pvu II from plasmid PUC 18. Lane 1, DNA control; lanes 2 to 4, calicheamicin γ_1^I at 10, 1, and 0.1 μg/ml, respectively. Preferred cleavage site 5′ C of TCCT shown with a solid line and arrow. Secondary cleavage sites 5′ C of ACCT and two nucleotides off toward the 3′ side of AGAG shown with dotted line and small arrow. (**B**) Cleavage of 125-bp fragment Eco RI–Bam HI containing 80-bp *Streptomyces* red promoter PCLL-pr7b (*9*). Reaction conditions and work-up are identical to those in (A). Lane 1, DNA control; lanes 2 to 4, calicheamicin γ_1^I at 1, 0.5, and 0.1 μg/ml, respectively. Preferred cleavage sites were at the 5′ T of CTCT and two nucleotides off toward the 3′ side of AGGA. Secondary cleavage site was two nucleotides in the direction of the 3′ side of AGGT.

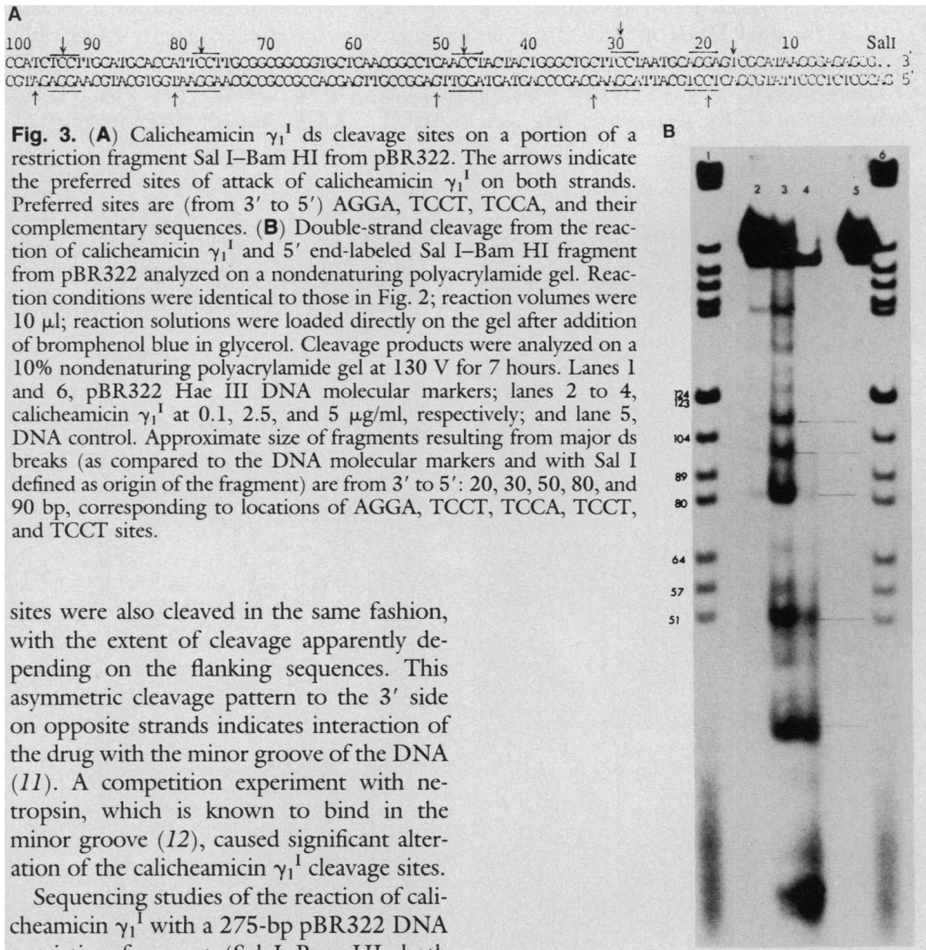

Fig. 3. (**A**) Calicheamicin γ_1^I ds cleavage sites on a portion of a restriction fragment Sal I–Bam HI from pBR322. The arrows indicate the preferred sites of attack of calicheamicin γ_1^I on both strands. Preferred sites are (from 3′ to 5′) AGGA, TCCT, TCCA, and their complementary sequences. (**B**) Double-strand cleavage from the reaction of calicheamicin γ_1^I and 5′ end-labeled Sal I–Bam HI fragment from pBR322 analyzed on a nondenaturing polyacrylamide gel. Reaction conditions were identical to those in Fig. 2; reaction volumes were 10 μl; reaction solutions were loaded directly on the gel after addition of bromphenol blue in glycerol. Cleavage products were analyzed on a 10% nondenaturing polyacrylamide gel at 130 V for 7 hours. Lanes 1 and 6, pBR322 Hae III DNA molecular markers; lanes 2 to 4, calicheamicin γ_1^I at 0.1, 2.5, and 5 μg/ml, respectively; and lane 5, DNA control. Approximate size of fragments resulting from major ds breaks (as compared to the DNA molecular markers and with Sal I defined as origin of the fragment) are from 3′ to 5′: 20, 30, 50, 80, and 90 bp, corresponding to locations of AGGA, TCCT, TCCA, TCCT, and TCCT sites.

sites were also cleaved in the same fashion, with the extent of cleavage apparently depending on the flanking sequences. This asymmetric cleavage pattern to the 3′ side on opposite strands indicates interaction of the drug with the minor groove of the DNA (*11*). A competition experiment with netropsin, which is known to bind in the minor groove (*12*), caused significant alteration of the calicheamicin γ_1^I cleavage sites.

Sequencing studies of the reaction of calicheamicin γ_1^I with a 275-bp pBR322 DNA restriction fragment (Sal I–Bam HI; both strands were 5′ and 3′ end-labeled) that is rich in TCCT-AGGA sequences (*13*) confirmed the preferred site of specific asymmetric cleavage (Fig. 3A). Furthermore, examination of the reaction mixture on a nondenaturing gel revealed excellent correlation between the observed ds cleavage sites and those cleaved sites observed on the denaturing gel (Fig. 3B). In the case of the TCCT sites, cutting reactions with the 5′ end-labeled strand indicated that calicheamicin γ_1^I breaks DNA at the 5′ Cs and to a lesser extent at the adjacent 5′ Ts. These reactions yielded fragments that exhibited electrophoretic mobilities identical to the corresponding chemically produced markers, thus suggesting the presence of 3′ phosphates at these breaks. However, when a 3′ end-labeled strand was cleaved (Fig. 4), two major drug-induced oligonucleotide products were observed that migrated on the gel as if they were one and two nucleotides longer than expected from the studies of 5′ end-labeled strands (Fig. 4, lane 1, bands a and b, respectively). Addition of EDTA to the cleaving reactions had no effect on the formation of product b but inhibited the formation of product a (Fig. 4, lane 2). Sodium hydroxide treatment of the EDTA-containing reaction products caused a shift in the migration of product b to a position on the gel (Fig. 4, lanes 3 and 4) where it matched the chemical marker corresponding to the 5′ C of the TCCT box (as was observed with the 5′ end-labeled strands). The alkaline treatment yields also product a in the same intensity as product b (Fig. 4, lanes 3 and 4).

These observations are consistent with the formation of 5′ termini ending in 5′ aldehyde nucleosides (product b) and 5′ carboxylic acid nucleosides (product a), a process (Fig. 5) first described by Goldberg and coworkers with neocarzinostatin, another diacetylene-containing antitumor agent (*14, 15*). Release of the terminal 5′ aldehyde nucleoside via a base-catalyzed β-elimination of its 3′ phosphate gives a polynucleotide fragment ending in 5′ phosphate, which comigrates on the gel with the corresponding chemical marker. To confirm these assignments, the EDTA-containing reaction products were further treated with sodium borohydride ($NaBH_4$); this caused the band corresponding to b to move slightly faster than the aldehyde band (Fig. 4, lane 5, band b′) as is consistent with the reduction of the 5′ aldehyde to the corresponding 5′ hydroxymethyl nucleoside. Product a (the 5′ carboxylic acid derivative) could be formed by further oxidation of the 5′ aldehyde, a reaction that was inhibited in presence of EDTA (Fig. 4, lane 2) and favored in the

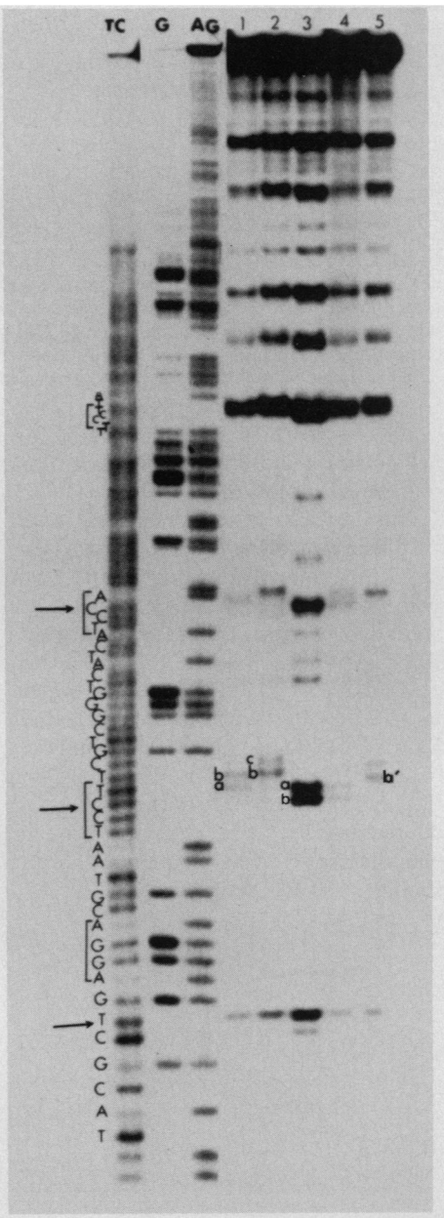

Fig. 4. Autoradiogram of high-resolution denaturing gel of calicheamicin γ_1^I cleavage of a 3′ end-labeled 275-bp Sal I–Bam HI fragment from pBR322. Incubation conditions were identical to those in Fig. 2 unless otherwise noted. Lane 1, calicheamicin γ_1^I at 0.5 μg/ml; lane 2, calicheamicin γ_1^I at 0.5 μg/ml in the presence of 1 m*M* EDTA; lanes 3 and 4, obtained after heating products of reaction identical to that of lane 2 in 0.1*M* NaOH at 90°C for 3 min (lanes 3 and 4 are identical except that lane 3 contained twice the amount of labeled DNA); and lane 5, obtained after treating reaction products from lane 2 with 0.28*M* $NaBH_4$ for 90 min; the DNA was precipitated and washed with ethanol after incubation with drug and prior to further treatment with NaOH or $NaBH_4$. TC, G, and AG are Maxam-Gilbert chemical sequencing lanes.

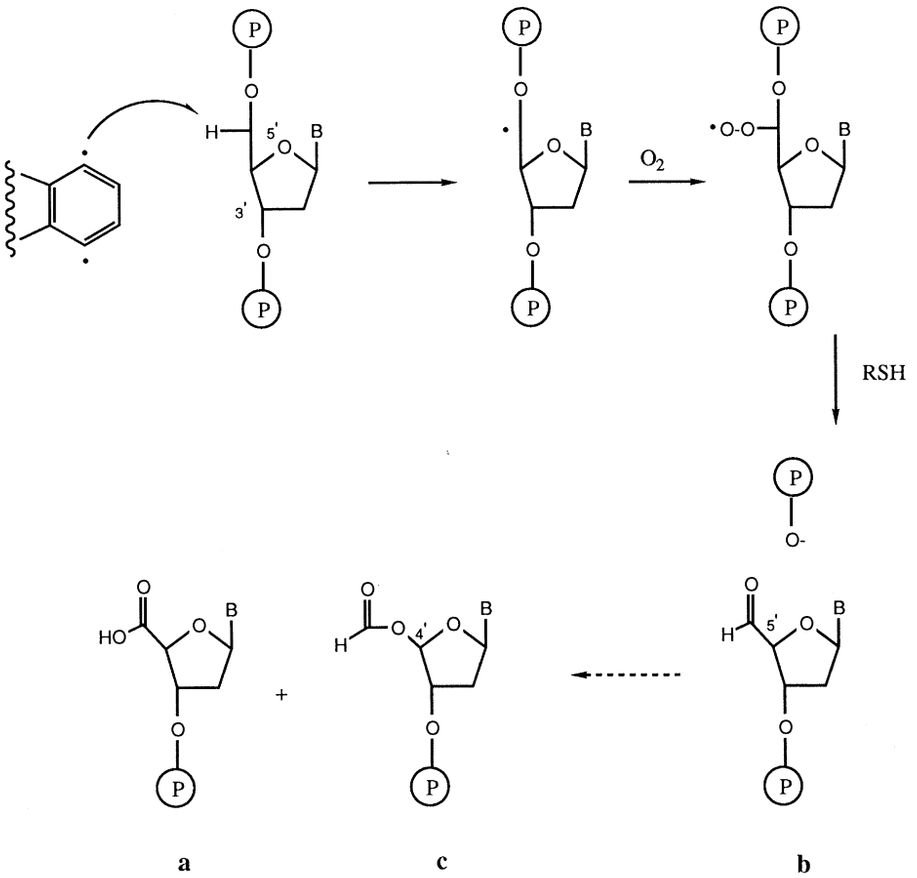

Fig. 5. Possible cleavage mechanism of the TCCT site at the 5′ C. A carbon-centered radical abstracts a 5′ hydrogen from the deoxyribose sugar. The sugar is then attacked by dioxygen to form a peroxyl radical, which in the presence of thiol (RSH) forms an aldehyde and causes strand scission. Aldehyde b could oxidize to the corresponding carboxylic acid a. It could also undergo a Baeyer-Villiger–like oxidative rearrangement to give the formate c.

presence of strong base (Fig. 4, lanes 3 and 4). When EDTA was added, an additional band (c) was observed, which could possibly represent the 5′ formate ester formed by oxygen insertion between C-4, and C-5, via a Baeyer-Villiger–like oxidative rearrangement on the aldehyde (*16*) (Fig. 5). This modified nucleoside would no doubt also be released by base treatment as observed in Fig. 4, lanes 3 and 4.

In contrast to the TCCT site, the electrophoretic mobility of the oligonucleotides produced by the reaction of calicheamicin γ_1^1 on the complementary AGGA site was not affected by base treatment. Whether the 5′ or the 3′ end-labeled strands were used, the cutting always occurred two bases toward the 3′ side of the AGGA box (Figs. 2B and 4). This result indicates the presence of intact phosphorylated 5′ and 3′ termini after strand scission.

Exclusion of oxygen from the reaction mixture inhibited strand scission, while the use of excess superoxide dismutase or catalase did not alter the DNA damage due to the drug (*17*). This suggests that neither superoxide radicals nor hydrogen peroxide are involved in the strand scission. The addition of ferrous ions had no effect on the cutting properties of the drug. The strand breaks in all of these reactions were remarkably specific, which argues against the presence of a diffusible radical species. Similar results have been observed with neocarzinostatin (*14, 15*) consistent with the mechanism depicted in Fig. 5 for the cleavage of the DNA at the TCCT sites. Neocarzinostatin, however, does not seem to recognize a specific sequence but instead produces single strand nicks almost exclusively at thymidylic and deoxyadenylic acid residues.

In conclusion, the staggered nature of the cleavage sites on the complementary strands of DNA and the unusual specificity of the cutting reaction suggests a unique fit of the drug and DNA. The partial insertion of the diyne-ene moiety into the minor groove where the diradical attacks the preferred sugars would account for the above findings. The physicochemical significance of the preferred cutting sites is unclear but seems to reflect some unique secondary structural feature related to the nucleotide sequence of the scission site and flanking regions (*18*).

REFERENCES AND NOTES

1. M. D. Lee *et al.*, *J. Am. Chem. Soc.* **109**, 3464 (1987).
2. M. D. Lee *et al.*, *ibid.*, p. 3466.
3. J. Golik *et al.*, *ibid.*, p. 3461.
4. J. Golik *et al.*, *ibid.*, p. 3462.
5. J. P. Thomas *et al.*, *26th Interscience Conference on Antimicrobial Agents and Chemotherapy*, New Orleans, LA, September 1986, abstract 229.
6. R. K. Elespuru and R. J. White, *Cancer Res.* **43**, 2819 (1983).
7. F. Durr and R. E. Wallace, American Cyanamid Co.—Medical Research Division, unpublished observations.
8. B. C. Fine of the American Cyanamid Agricultural Research Division, unpublished observations.
9. J. S. Feitelson, A. M. Sinha, E. A. Coco, *J. Nat. Prod.* **49**, 998 (1986).
10. A. M. Maxam and W. Gilbert, *Methods Enzymol.* **65**, 499 (1980).
11. J. P. Sluka, S. J. Horvath, M. F. Bruist, M. I. Simon, P. B. Dervan, *Science* **238**, 1129 (1987).
12. M. L. Kopka, C. Yoon, D. Goodsell, P. Pjura, R. E. Dickerson, *Proc. Natl. Sci. U.S.A.* **82**, 1376 (1985).
13. T. Maniatis, E. D. Fritsch, J. Sambrook, *Molecular Cloning: A Laboratory Manual* (Cold Spring Harbor Laboratory, Cold Spring Harbor, NY, 1982), p. 480.
14. L. S. Kappen and I. H. Goldberg, *Biochemistry* **22**, 4872 (1983); L. S. Kappen, T. E. Ellenberger, I. H. Goldberg, *ibid.* **26**, 384 (1987); K. Edo *et al.*, *Tetrahedron Lett.* **26**, 331 (1985); O. D. Hensens *et al.*, *Biochem. Biophys. Res. Commun.* **113**, 538 (1983); A. G. Myers, *Tetrahedron Lett.* **28**, 4493 (1987).
15. I. H. Goldberg, *Free Radical Biol. Med.* **3**, 41 (1987).
16. J. March, *Advanced Organic Chemistry* (Wiley, New York, 1985), pp. 990 and 1073.
17. N. Zein, A. M. Sinha, W. J. McGahren, G. A. Ellestad, unpublished data.
18. R. E. Dickerson and H. R. Drew, *J. Mol. Biol.* **149**, 761 (1981).

19. We thank M. Greenstein, J. Feitelson, and D. Rothstein for helpful discussions and W. Maiese for encouragement and support.

21 December 1987; accepted 11 March 1988